Journal for
ImmunoTherapy of Cancer

Restoration of miR-340 controls pancreatic cancer cell *CD47* expression to promote macrophage phagocytosis and enhance antitumor immunity

Qing Xi,[1] Jieyou Zhang,[1] Guangze Yang,[1] Lijuan Zhang,[1] Ying Chen,[2] Chengzhi Wang,[1] Zimu Zhang,[1] Xiangdong Guo,[1] Jingyi Zhao,[2] Zhenyi Xue,[1] Yan Li,[1] Qi Zhang,[3] Yurong Da,[1] Li Liu,[4] Zhi Yao,[1] Rongxin Zhang ![ORCID][5]

For numbered affiliations see end of article.

Correspondence to
Professor Rongxin Zhang; rongxinz@yahoo.com

ABSTRACT

Background Immune checkpoint blockade has emerged as a potential cancer immunotherapy. The "don't eat me" signal *CD47* in cancer cells binds signal regulatory protein-α on macrophages and prevents their phagocytosis. The role of miR-340 in pancreatic ductal adenocarcinoma (PDAC), especially in tumor immunity, has not been explored. Here, we examined the clinical and biological relevance of miR-340 and the molecular pathways regulated by miR-340 in PDAC.

Methods *CD47* and miR-340 expression and the relationship with cancer patient survival were analyzed by bioinformatics. The mechanism of miR-340 action was explored through bioinformatics, luciferase reporter, qRT-PCR and western blot analyses. The effects of miR-340 on cancer cells were analyzed in terms of apoptosis, proliferation, migration and phagocytosis by macrophages. *In vivo* tumorigenesis was studied in orthotopic and subcutaneous models, and immune cells from the peripheral and tumor immune microenvironments were analyzed by flow cytometry. Depletion of macrophages was used to verify the role of macrophages in impacting the function of miR-340 in tumor progression.

Results miR-340 directly regulates and inversely correlates with *CD47*, and it predicts patient survival in PDAC. The restoration of miR-340 expression in pancreatic cancer cells was sufficient to downregulate *CD47* and promote phagocytosis of macrophages, further inhibiting tumor growth. The overexpression of miR-340 promoted macrophages to become M1-like phenotype polarized in peripheral and tumor immune microenvironments and increased T cells, especially CD8$^+$ T cells, contributing to the antitumor effect of miR-340.

Conclusions miR-340 is a key regulator of phagocytosis and antitumor immunity, and it could offer a new opportunity for immunotherapy for PDAC.

INTRODUCTION

Pancreatic ductal adenocarcinoma (PDAC) continues to be one of the most lethal cancers with a 5-year survival rate of 8%.[1] Even after a potentially radical resection, most patients eventually relapse.[2] In addition, the tumor biology of PDAC contributes to early recurrence, metastasis and resistance to chemotherapy and radiotherapy. Several treatments such as gemcitabine, FOLFIRINOX and nab-paclitaxel are able to moderately extend the median survival of PDAC, but they have limited efficacy in producing significant improvements. Therefore, the development of new effective treatments is urgently needed.

The blockade of *CD47* is an active research area of tumor immunotherapy, which is one of the most promising advances in oncology.[34] As a transmembrane protein, *CD47* functions as a ligand for signal-regulated protein-α (*SIRPα*) and is widely expressed on all normal cells and overexpressed on tumor cells.[5] The binding of *CD47* to *SIRPα* initiates a signaling cascade that coupling of *SIRPα* to inhibitory molecules, such as src homology-2 (SH2)-domain containing protein tyrosine phosphatases-1 (SHP-1) and SHP-2, thereby transmits a "don't eat me" signal to prevent phagocytosis.[6–8] The blockade of *CD47–SIRPα* axis with anti-*CD47* antibodies could greatly enhance the ability of macrophages to engulf both hematological tumor cells and solid tumor cells.[9–12] However, the mechanism by which *CD47–SIRPα* blockade promotes antitumor immunity remains unclear at both the molecular and immunological levels. An understanding of these mechanisms will likely help the design of optimal therapeutic strategies for improving the efficacy of current treatments for patients suffering from PDAC.

MicroRNAs (miRNAs) represent a class of evolutionarily conserved small non-coding RNAs that play crucial roles in lots of aspect in biology by binding to its complementary target mRNAs.[13 14] Growing evidences support the role of miRNAs in development and disease, especially cancer. In addition,

accumulating studies have suggested a significant role of miRNAs in regulation of the immune response[15 16] and have emerged as attractive targets for novel therapeutic approaches.[17 18] Several miRNAs regulate *CD47* in various cancers, such as miR-133a[19] and miR-708.[20] Therefore, the identification of novel miRNAs acting as regulators of antitumor immunity might reveal potential targets for cancer immunotherapy.

Previous studies showed that miR-340 was involved in tumor suppression through the regulation of expression of genes related with tumor progression,[21 22] however few studies of miR-340 on antitumor immunity were reported. In this study, we identified miR-340 as a novel miRNA that predicts the cancer patient survival in PDAC, and demonstrated that miR-340 increased macrophage-mediated phagocytosis by downregulating *CD47* on pancreatic cancer cells, consequently enhancing antitumor immunity.

MATERIALS AND METHODS
Detailed methods can be found in the online supplementary materials and methods.

Animals
C57BL/6 mice were purchased from the Academy of Military Medical Science (Beijing, China). All the mice used were 6–8 weeks old and housed in a specific pathogen-free animal facility at the Experimental Animal Center of Tianjin Medical University (Tianjin, China). The care and treatment for mice were performed according to guidelines for Laboratory Animal care and were approved by the Animal Ethics Committee of Tianjin Medical University (Tianjin, China).

Cell culture
Mouse pancreatic cancer cell line Panc02 and human pancreatic cancer cell line PANC1 were originally obtained from American Type Culture Collection. These cells were cultured in medium containing Dulbecco's Modified Eagle Medium (DMEM), 10% fetal bovine serum (FBS), 100 U/mL penicillin and 100 μg/mL streptomycin, and incubated at 37°C in a humidified atmosphere with 5% CO_2.

Luciferase reporter assays
The 3′ UTR of wild type (wt) or mutant *CD47* were synthesized and cloned into pmirGLO dual-luciferase miRNA target expression vector (Promega). The pmirGLO dual-luciferase 3′ UTR vectors were cotransfected with miR-340 overexpression vector into 293 T cells. The cells were harvested and lysed 48 hours after transfection. The luciferase activity was measured by a dual-luciferase assay system (Promega).

Orthotopic model of PDAC
To establish the orthotopic model of PDAC, mouse abdomens were prepared with betadine solution, and an approximately 1 cm wide incision was performed in the upper left of each abdomen. The tip of the pancreas was gently grasped, and the pancreas and spleen were externalized in the lateral direction to expose them completely. A needle was inserted into the pancreas tail and positioned in the pancreatic head region. Then, 2×10^6 Panc02 cells stable overexpression of miR-NC or miR-340 suspended in 50 μL phosphate buffered saline (PBS) were slowly injected using an insulin injection needle. The spleen was restored to the appropriate position in the abdomen, and the skin and peritoneum were closed with 3-0 vicryl sutures. After 3 weeks, all mice were euthanized, and the tumor tissues were collected for further study.

Subcutaneous model of PDAC
Panc02 cells stable overexpression of miR-NC or miR-340 were washed three times with PBS, and 2×10^6 cells suspended in 100 μL PBS were subcutaneously injected into the dorsal part of the mice. From day 10, the tumor size was measured every 2 days and tumor volume was calculated as length × width^2/2. Mice with tumors larger than 20 mm in size at the longest axis were euthanized due to ethical considerations. To analyze the effect of miR-340 on tumor growth, all mice were euthanized for further study.

Flow cytometry analysis
For *in vivo* experiments, the tumors were weighed and digested at 37°C in 10 mL digestion solution (PBS supplemented with type I collagenase (200 U/mL), hyaluronidase and DNase I (100 μg/mL)) for 1 hour. Single cell suspensions were obtained by grinding the digested tissues and filtering through a 70 μm cell strainer (Becton and Dickinson, BD, USA). The immune cells were freshly isolated using density gradient centrifugation and stained with antibodies for 30 min at 4°C. The following monoclonal anti-mouse antibodies were used: CD45-PECy5.5 (eBioscience, USA), CD3-PECy7 (eBioscience, USA), CD4-APC (BioLegend, USA), CD8-APC (eBioscience, USA), F4/80-APC (Sungene, China), CD11b-PECy7 (eBioscience, USA) and MHC II-PE (eBioscience, USA). Flow cytometry was performed and the data were analyzed using FlowJo software (TreeStar, Ashland, Oregon, USA).

Generation of macrophages and *in vitro* phagocytosis assay
To obtain macrophages from the peritoneal cavity, thioglycollate-elicited peritoneal macrophages were collected 96 hours after an intraperitoneal injection of a 3% thioglycollate solution. The cells were harvested from the peritoneal cavity in 10 mL of PBS and cultured in Roswell Park Memorial Institute (RPMI)-1640 supplemented with 10% FBS and 1% penicillin–streptomycin for 2 hours at 37°C with 5% CO_2 to macrophages. Then the non-adherent cells were removed. To obtain macrophages from the bone marrow, bone marrow cells were isolated from the femur and tibia of C57BL/6 mice and cultured in complete RPMI-1640 medium supplemented with 10 μg/mL recombinant mouse M-CSF (PeproTech) in a CO_2 incubator for 5 days at 37°C to differentiate into

macrophages. The cells were washed twice every other day with PBS and then cultured with fresh medium. The macrophages acquired from both the peritoneal cavity and bone marrow (5×10^4 per well) were separately seeded in 24-well culture plates in complete RPMI-1640 medium for 24 hours prior to the experiment. The macrophages were incubated in serum-free medium for 2 hours, and 2×10^4 GFP$^+$ cancer cells were added. After co-cultivation at 37°C for 4 hours, the cells were harvested, and the macrophages were stained with macrophage antibody anti-mouse F4/80-APC (Sungene, China); then, the phagocytosis was inspected using a Fluoview FV1000 Laser Scanning Confocal Microscope (Olympus, Japan). The phagocytosis was calculated as the number of phagocytosed GFP$^+$ cells per 100 macrophages. For the flow cytometry analysis of phagocytosis, 10,000 cells per sample were analyzed using a FACS Canto II flow cytometer (BD, USA), and unstained control and single stained cells were prepared for gating. Phagocytosis was calculated as the percentage of F4/80$^+$GFP$^+$ cells among F4/80$^+$ macrophages.

In vivo antibody blocking
The orthotopic model of PDAC was established in accordance with protocols described previously. In brief, C57BL/6 mice were injected with 2×10^6 Panc02 cells stable overexpression of miR-NC or miR-340 into the pancreas. Tumors were allowed to grow for 7–10 days and treated with isotype control IgG (200 µg/day intravenously, Clone No. MPC-11, BioXcell) or anti-mouse *CD47* mAb (200 µg/day intravenously, Clone No. MIAP301, BioXcell) *in vivo*. After 2 weeks of treatment, the mice were sacrificed, and tumors were removed and digested to perform flow cytometry. The phagocytosis was calculated as the percentage of F4/80$^+$GFP$^+$ cells among CD11b$^+$F4/80$^+$ macrophages.

Macrophage depletion studies
The depletion of macrophages in C57BL/6 mice was performed as previously described[23] with minor modifications. In brief, the mice were injected intravenously with 200 µL of either clodronate liposomes or control liposomes (Clodronateliposomes.com, Amsterdam, The Netherlands) 1 day before *in situ* injections of miR-NC or miR-340 overexpression Panc02 cells into the pancreas, and then the tumor-bearing mice were injected intravenously with 200 µL of the respective liposomes every 3 days. After performing the depletion protocol six times, the mice were sacrificed for further study. The effectiveness of the macrophage depletion was determined by a flow cytometry analysis of the percentage of macrophages (CD45$^+$CD11b$^+$F4/80$^+$) among splenocytes or tumor-infiltrating cells.

Bioinformatics analysis
The candidate targeting miRNAs of *CD47* were derived from integrated miRNA target prediction algorithms (miRanda,[24] DIANA-microT[25] and TargetScan[26]). The clinical relevance of *CD47* and miR-340 was confirmed by data from the Oncomine (https://www.oncomine.org)[27] and LinkedOmics (http:// www.linkedomics.org).[28]

Statistical analysis
The statistical analysis was performed by two-tailed unpaired Student's t-test or two-way Analysis of Variance (ANOVA) and presented as the mean±SEM using the Prism software (GraphPad, USA). The correlation was evaluated by Spearman's correlation analysis. The log-rank Mantel–Cox test was used for survival analysis. The differences were considered significant at p<0.05.

RESULTS
MiR-340 is negatively correlated with the expression of *CD47* in multiple cancers and significantly associated with PDAC
First, we evaluated the expression of *CD47* in primary human tissues from "normal" adjacent non-tumor pancreas and PDAC tissues from the Oncomine database. Although *CD47* was still detectable in the normal (non-tumor) pancreatic tissues, the expression of *CD47* in primary PDAC tissues was significantly higher (p<0.001) (figure 1A). Then, we explored whether *CD47* was a prognostic factor of PDAC. In the Cox regression analysis performed with LinkedOmics, the stratification of patients into "*CD47* high" and "*CD47* low" groups based on the median expression revealed that high levels of *CD47* expression were associated with decreased probability of survival in PDAC (figure 1B). To explore the potential regulation of *CD47* by miRNAs, we used miRNA target-predicting algorithms (miRanda, DIANA-microT and TargetScan) based on the presence of binding sites in the 3′ UTR and found eight candidate miRNAs that overlapped among these algorithms (figure 1C). Then, we used LinkedOmics to identify miRNAs that were significantly inversely correlated with *CD47* expression in three cancers, namely, PDAC, lung adenocarcinoma (LUAD) and skin cutaneous melanoma (SKCM), and explored three candidate miRNAs that overlapped among the three kinds of cancers (figure 1D). As shown in figure 1E–G, miR-340 was inversely correlated with *CD47* in 32 LUAD samples, 97 SKCM samples and 178 PDAC samples. In addition, the heat map showed that miR-340 ranked as the fourth most significantly negatively correlated miRNA with *CD47* expression in PDAC (figure 1H). These findings indicated that miR-340 may be closely related to pancreatic cancer development and progression. To determine the expression of miR-340 and its correlation with the prognosis of PDAC, we analyzed data from starBase and found that the expression of miR-340 in primary PDAC tissues was significantly lower than that in normal pancreatic tissues (figure 1I). Low expression of miR-340 was associated with a decreased probability of overall survival in PDAC (figure 1J). MiR-340 was significantly increased following radiation therapy in patients suffering from PDAC (figure 1K). These results indicated
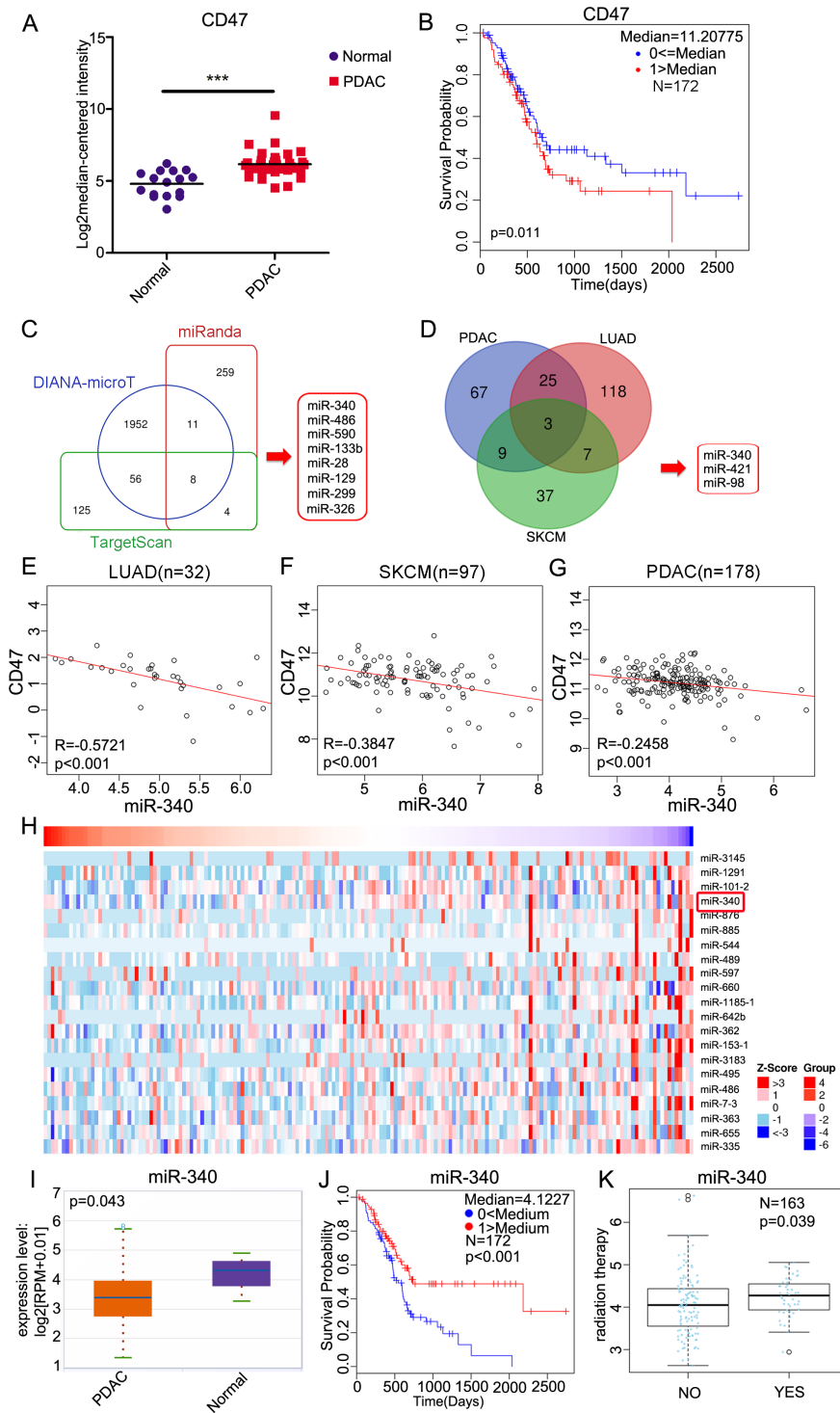
Figure 1 miR-340 is negatively correlated with the expression of *CD47* and overall survival in PDAC. (A) Analyses of *CD47* expression in normal pancreas (n=16) and pancreatic carcinoma tissues (n=36) by the Oncomine database (p<0.001). (B) The Cox regression analysis revealed a correlation between higher *CD47* expression and a poorer prognosis in 172 patients with PDAC analyzed using the LinkedOmics database (p=0.011). (C) Bioinformatics predictions of miRNAs targeting *CD47* by miRanda, DIANA-microT and TargetScan. (D) LinkedOmics-identified miRNAs that were significantly negatively correlated with *CD47* in PDAC, LUAD and SKCM. (E) The correlative analysis of miR-340 and *CD47* in human LUAD (n=32), (F) SKCM (n=97) and (G) PDAC (n=178). (H) Heat map of miRNAs that were negatively correlated with *CD47* in PDAC. (I) Analyses of miR-340 expression in normal pancreas (n=4) and pancreatic carcinoma tissues (n=178) by starBase (p=0.043). (J) Cox regression analysis performed using the LinkedOmics database revealed a correlation between miR-340 and survival probability in 172 patients suffering from PDAC (p<0.001). (K) Graphs show the impact of radiation therapy on the expression of miR-340 in PDAC (p=0.039). The data in A and I were analyzed by two-tailed, unpaired t-test. The data in B and J were analyzed by the log-rank Mantel–Cox test. Spearman correlation analysis was used in E–G. The data in K were analyzed using a two-sided Wilcox test. LUAD, lung adenocarcinoma; PDAC, pancreatic ductal adenocarcinoma; SKCM, skin cutaneous melanoma.

that miR-340 may be a clinically relevant prognostic factor and plays critical roles in PDAC.

CD47 is a direct target of miR-340

Evaluation of the 3′ UTR sequence of *CD47* revealed one binding site with a perfectly matched sequence for miR-340. To confirm the existence of a direct relationship between miR-340 and its predicted target *CD47*, we cloned the 3′ UTR of *CD47* into the dual-luciferase vector pmirGLO and generated mutations in the binding site to abrogate the interaction between miR-340 and the *CD47* 3′ UTR. As expected, while the reporter with the intact *CD47* 3′ UTR was effectively suppressed by miR-340, the *CD47* 3′ UTR carrying a mutated binding site was resistant to suppression by miR-340 (figure 2A). Additionally, we overexpressed miR-340 by transfecting miR-340 mimics into the mouse pancreatic cancer cell line Panc02, and the efficiency of the overexpression was confirmed by Quantitative Real-time PCR (qRT-PCR). We found that the overexpression of miR-340 by mimic transfection significantly decreased *CD47* at both the mRNA and protein levels in Panc02 cells (figure 2B). Then, we constructed Panc02 cells with stable miR-NC and miR-340 stable overexpression, and the high expression efficiency was confirmed by qRT-PCR. We determined that, consistent with the effect of the miR-340 mimics, the stable overexpression of miR-340 could also notably decrease the expression of *CD47* in Panc02 cells (figure 2C). To further confirm the regulation of *CD47* by miR-340 in human pancreatic cancer cells, we overexpressed miR-340 by transfecting miR-340 mimics into the human pancreatic cancer cell line PANC1. We confirmed the overexpression of miR-340 by qRT-PCR and found that the overexpression of miR-340 by mimic transfection significantly decreased the expression of *CD47* in PANC1 cells (figure 2D). Taken together, these results indicate that miR-340 downregulates *CD47* through a binding site in its 3′ UTR.

High expression of miR-340 does not directly affect apoptosis, proliferation or migration of cancer cells

To explore the effect of miR-340 on the biological function of mouse pancreatic cancer cells, we detected the effect of both miR-NC and miR-340 stable overexpression on Panc02 cell apoptosis with Annexin-V/7-AAD and flow cytometry, and no significant difference was found between the two groups (figure 2E). We also explored the proliferation of Panc02 cells with stable overexpression of miR-NC or miR-340 with the CCK-8 assay at 0, 24, 48, 72 and 96 hours and found no clear difference in proliferation (figure 2F). To detect the impact of miR-340 on the migration of Panc02 cells, we performed a wound healing assay. As shown in figure 2G, there were no obvious changes in wound healing. To explore the effect of miR-340 on the biological function of human pancreatic cancer cells, we overexpressed miR-340 by transfecting miR-340 mimics into PANC1 cells and detected cell apoptosis with Annexin-V/PI by flow cytometry. No significant difference was found between the two groups (figure 2H).
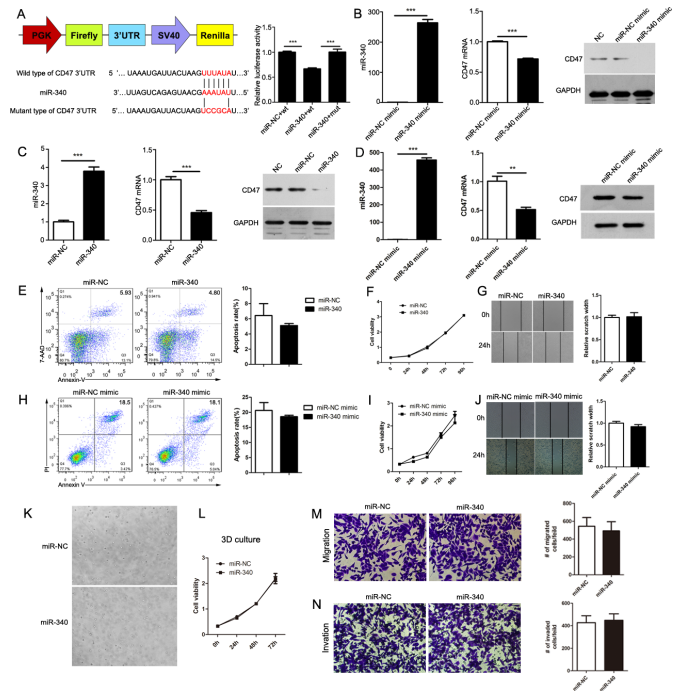

Figure 2 *CD47* is a direct target of miR-340. (A) Activity of luciferase reporters and Renilla plasmids containing wild type (wt) or mutant (mut) *CD47* 3′ UTRs that were cotransfected with miR-340 overexpression vector or respective controls. (B) The expression of miR-340 and *CD47* in control mimic-transfected or miR-340 mimic-transfected Panc02 cells. (C) The expression of miR-340 and *CD47* in Panc02 cells with stable miR-NC or miR-340 overexpression. (D) The expression of miR-340 and *CD47* in control mimic-transfected or miR-340 mimic-transfected PANC1 cells. miR-340 and *CD47* expression were normalized to *U6* small nuclear RNA and *GAPDH* levels, respectively. (E) Overexpression of miR-340 does not affect the apoptosis of Panc02 cells. (F) Overexpression of miR-340 does not affect the proliferation of Panc02 cells. (G) Overexpression of miR-340 does not affect the migration of Panc02 cells. (H) Overexpression of miR-340 does not affect the apoptosis of PANC1 cells. (I) Overexpression of miR-340 does not affect the proliferation of PANC1 cells. (J) Overexpression of miR-340 does not affect the migration of PANC1 cells. (K) Representative images of cell growth using hydrogel VitroGel 3D. (L) Statistical analysis of differences in proliferation between miR-NC and miR-340 Panc02 cells in VitroGel 3D. (M) Overexpression of miR-340 does not affect the migration of Panc02 cells in VitroGel 3D. (N) Overexpression of miR-340 does not affect the invasion of Panc02 cells in VitroGel 3D. Representative images were taken at 4× magnification. The error bars were shown as mean±SEM and the significance was calculated using a two-tailed, unpaired t-test. **P<0.01 and ***p<0.001. Data were representative of one of three independent experiments.

We also explored the proliferation of miR-NC-transfected or miR-340 mimic-transfected PANC1 cells with the CCK-8 assay at 0, 24, 48, 72 and 96 hours and there was no clear difference (figure 2I). Similarly, no obvious impact of miR-340 on the migration of PANC1 cells was observed (figure 2J). As 2D culture does not reproduce important tumor-enriched metabolic states, we explored the impact

of miR-340 on tumor cell growth in VitroGel 3D, a hydrogel similar to Matrigel. We detected the proliferation of Panc02 cells with stable overexpression of miR-NC or miR-340 with the CCK-8 assay at 0, 24, 48 and 72 hours in VitroGel 3D. Representative images of cell growth in 3D culture are shown in figure 2K, and there was no clear difference in cell viability in 3D culture (figure 2L). Then we evaluated the ability of cells in VitroGel to migrate through the 24-well cell culture inserts with or without the hydrogel VitroGel 3D. The 3D migration and invasion assays showed that overexpression of miR-340 did not impact either the migration or invasion of Panc02 cells in VitroGel 3D (figure 2M,N). Overall, the high expression of miR-340 did not directly affect apoptosis, proliferation, migration or invasion of pancreatic cancer cells.

High expression of miR-340 significantly promotes phagocytosis of tumor cells by macrophages

CD47-mediated *CD47–SIRPα* signaling plays important roles in phagocytosis by human and mouse macrophages in different types of hematologic and solid cancers.[3 29] As we have demonstrated that *CD47* is the direct target of miR-340, we attempted to explore the impact of miR-340 on the ability of macrophages to engulf cancer cells. First, we isolated macrophages from the mouse peritoneal cavity and then cocultured these macrophages with Panc02 cells stably overexpressing miR-NC or miR-340. After 4 hours, the cells were harvested and stained with anti-mouse F4/80-APC, and flow cytometry was performed. The results clearly showed that compared with that of miR-NC Panc02 cells, the phagocytosis of Panc02 cells with stable overexpression of miR-340 by mouse peritoneal cavity-derived macrophages was significantly increased (figure 3A,B). The gating strategy is shown in online supplementary figure S1. Then, we performed *in vitro* phagocytosis assays by incubating bone marrow-derived macrophages (BMDMs) with Panc02 cells stably overexpressing miR-NC or miR-340. As expected, we found that the forced expression of miR-340 increased the level of phagocytosis by approximately twofold compared with that in the miR-NC group (figure 3C,D). We also used an anti-*CD47* antibody to block *CD47*, and the results showed that overexpression of miR-340 significantly increased the phagocytosis by macrophages with *CD47* blockade (figure 3E,F). Furthermore, we performed *in vitro* phagocytosis assays by incubating BMDMs with Panc02 cells stably overexpressing miR-NC or miR-340, with or without *CD47* blocking, and measured phagocytosis by fluorescence microscopy. Representative images of Panc02 cell coculture groups with stable overexpression of both miR-NC and miR-340 were acquired. The white arrows indicate macrophages that engulfed cancer cells. The overexpression of miR-340 significantly increased the phagocytosis by macrophages, and phagocytosis was further increased when *CD47* was blocked (figure 3G,H, online supplementary figure S2). These results indicated that miR-340 may serve as a potent therapeutic target against PDAC given its close relationship with macrophage phagocytosis.
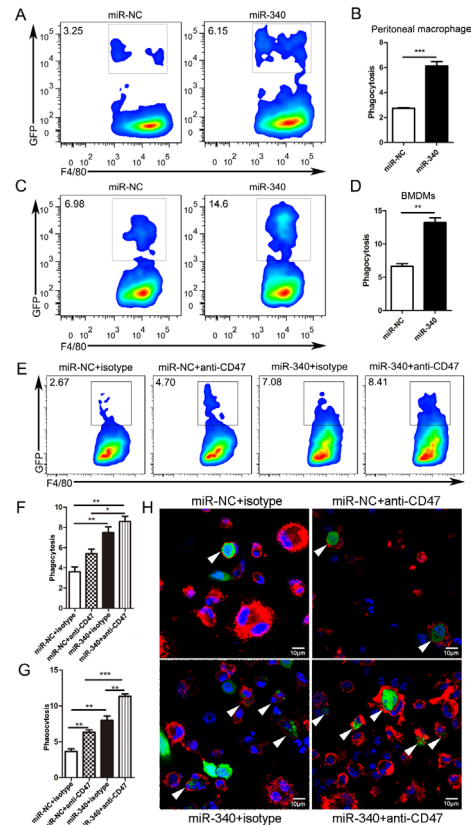
Figure 3 Overexpression of miR-340 promotes phagocytosis of tumor cells by macrophages. Panc02 cells overexpressing miR-NC or miR-340 were incubated with mouse peritoneal cavity-derived macrophages or BMDMs for 4 hours, stained with F4/80-APC antibody and analyzed by flow cytometry. Phagocytosis was described as the percentage of F4/80⁺GFP⁺ phagocytosed cancer cells by F4/80⁺ macrophages. (A, C) Representative plots show the percentage of F4/80⁺GFP⁺ macrophages phagocytosing cancer cells among F4/80⁺ peritoneal cavity-derived macrophages and BMDMs. (B, D) Statistical analysis of phagocytosis of pancreatic cancer cells by both peritoneal cavity-derived macrophages and BMDMs. (E) Representative plots show the percentage of F4/80⁺GFP⁺ macrophages phagocytosing cancer cells among F4/80⁺ BMDMs treated with isotype control or *CD47* blocking antibody. (F) Statistical analysis of phagocytosis of Panc02 cells by BMDMs with or without *CD47* blocking by flow cytometry. Panc02 cells overexpressing miR-NC or miR-340 were incubated with BMDMs for 4 hours, stained with F4/80-APC antibody and analyzed by immunofluorescence staining. (G) Statistical analysis of phagocytosis of Panc02 cells by BMDMs treated with isotype control or *CD47* blocking antibody for immunofluorescence staining. (H) Immunofluorescence staining shows representative images of mouse BMDMs engulfing Panc02 cells with miR-NC and miR-340 overexpression with or without *CD47* blocking. The white arrows point to macrophages that phagocytose cancer cells. Macrophages were stained red (F4/80⁺), cancer cells were green (GFP⁺) and nuclei were blue (DAPI⁺). Magnification: 100×. The error bars were shown as mean±SEM and the data were analyzed by two-tailed, unpaired t-test. *P<0.05; **p<0.01 and ***p<0.001. The experiments were performed three times with similar results. BMDM, bone marrow-derived macrophages.
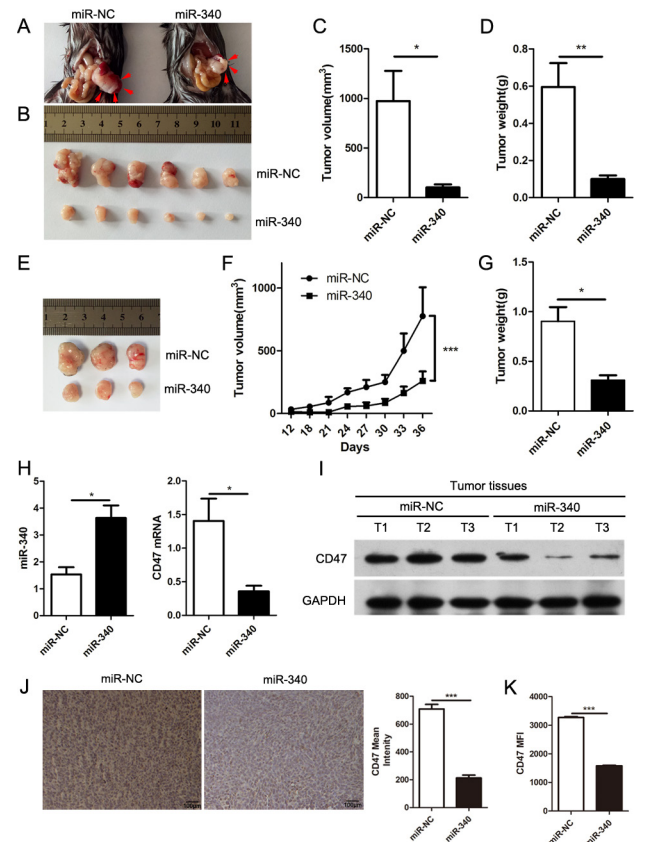
## Overexpression of miR-340 inhibits tumor growth *in vivo*

To determine whether the forced expression of miR-340 might exert suppressive effects on cancer development, we further performed an experiment using an orthotopic model of PDAC. C57BL/6 mice were implanted with Panc02 cells stably overexpressing miR-NC or miR-340 through direct injection into the pancreas. Compared with the miR-NC Panc02 cell-implanted mice, the miR-340 stable overexpression Panc02 cell-implanted mice exhibited a significantly reduced tumor size (figure 4A–C) and tumor weight (figure 4D). Furthermore, we performed an experiment using a subcutaneous mouse model of PDAC. C57BL/6 mice were subcutaneously inoculated with Panc02 cells stably overexpressing miR-NC or miR-340 into the shaved right lateral flanks. Consistent with the results obtained using the orthotopic mouse model, this model showed that compared with the tumors in the miR-NC Panc02 cell-implanted mice, the overexpression of miR-340 significantly reduced both the tumor volume (figure 4E,F) and tumor weight (figure 4G). In addition, we detected the expression of miR-340 and *CD47* in orthotopic tumors from both the miR-NC and miR-340 stable overexpression Panc02 cell-bearing mice and found that *CD47* was obviously downregulated in the tumors of the miR-340 overexpression group both at the mRNA (figure 4H) and protein levels (figure 4I). We also performed immunohistochemistry and flow cytometry, and the mean intensity and the mean fluorescence intensity (MFI) of *CD47* in mice bearing Panc02 cells stably overexpressing miR-NC or miR-340 confirmed that the expression of *CD47* was decreased in tumors in the miR-340 overexpression group (figure 4J,K). These results indicated that miR-340 may function as a tumor suppressor by targeting *CD47*.

Overexpression of miR-340 markedly enhances antitumor immunity

To determine whether miR-340 could enhance antitumor immunity *in vivo*, tumor-infiltrating immune cells from mice bearing Panc02 cells stably overexpressing miR-NC or miR-340 were stained and assessed via flow cytometry. Compared with that in the miR-NC Panc02 cell-bearing mice, the percentage and MFI of the M1-like (CD11b^{+}F4/80^{+}MHC-II^{+}) phenotype in the tumors were significantly increased in the miR-340 stable overexpression group (figure 5A). The ratio of M1-like and M2-like cells in the tumors from the miR-340 stable overexpression group was dramatically increased (figure 5B). Consistent with the changes in tumors, the percentages and MFI of the M1-like phenotype in the spleens of mice bearing Panc02 cells overexpressing miR-340 were obviously increased (figure 5C). The M1-like and M2-like cell ratio in the spleens in the miR-340 stable overexpression group was markedly increased (figure 5D). Although the CD4^{+} T lymphocytes showed no statistically significant difference between the tumors from mice bearing Panc02 cells with stable overexpression of miR-NC or miR-340 (figure 5E), the CD8^{+} T lymphocytes were significantly

Figure 4 High expression of miR-340 inhibits the growth of tumors. Panc02 cells stably overexpressing miR-NC or miR-340 were injected into the pancreas. Mice were euthanized 3 weeks after *in situ* tumor growth. Representative quantitation and images were shown from three separate experiments with at least six mice per group (A–D). (A–B) Representative images of tumors from mice bearing Panc02 cells overexpressing miR-NC and miR-340. The tumors were outlined by red arrows. (C) Final tumor volumes. (D) Final tumor weights. Panc02 cells stably overexpressing miR-NC or miR-340 were injected subcutaneously into mice and euthanized 36 days after tumor transplantation (n=3 per group) (E–G). (E) Representative images of tumors from miR-NC and miR-340 stable overexpression Panc02 cell-bearing mice. (F) Tumor growth curves. (G) Final tumor weights. (H) qRT-PCR analyses of the expression of miR-340 and *CD47* in orthotopic pancreatic cancer tissues of miR-NC or miR-340 stable overexpression Panc02 cell-bearing mice (n=3 per group). (I) The expression of *CD47* in tumors of miR-NC and miR-340 stable overexpression Panc02 cell-bearing mice (n=3 per group). (J) The mean intensity of *CD47* in tumors from miR-NC or miR-340 stable overexpression Panc02 cell-bearing mice analyzed by immunohistochemistry. Scale bar, 100 μm. (K) The mean fluorescence intensity of *CD47* in miR-NC or miR-340 stable overexpression Panc02 cell-bearing mice analyzed by flow cytometry. Representative quantitation was shown from three separate experiments with at least three mice per group. The error bars were shown as mean±SEM. Two-tailed, unpaired t-test was used in C, D, G, H, J and K. Two-way ANOVA was used in F. *P<0.05; **p<0.01 and ***p<0.001. The data were representative of three independent experiments.
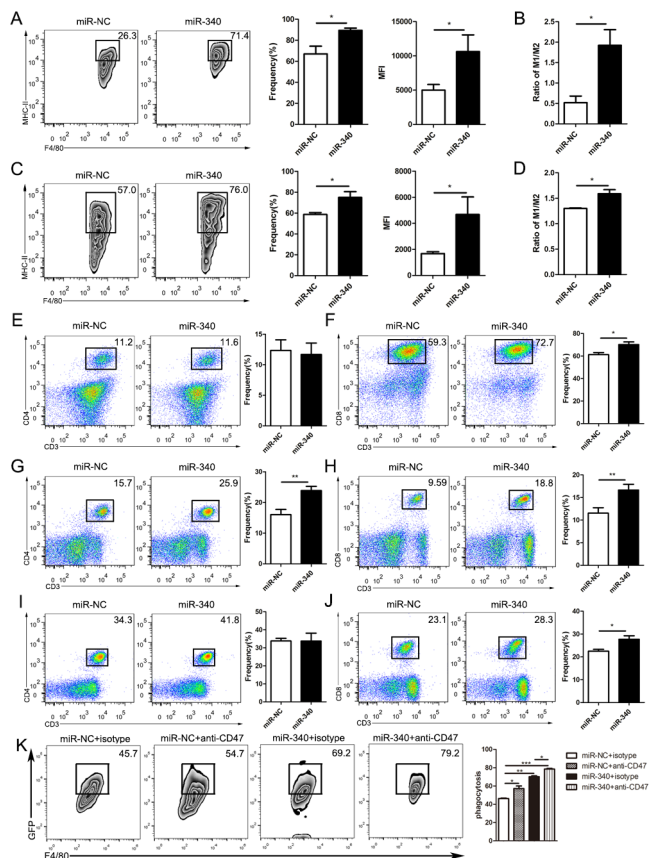
Figure 5 High expression of miR-340 notably enhances antitumor immunity. An orthotopic model of PDAC was built with Panc02 cells stably overexpressing miR-NC or miR-340, and the tumor and peripheral immune microenvironment were analyzed by flow cytometry 3 weeks after orthotopic implantation (n=7 per group). (A) The frequency and MFI of M1-like (CD11b$^+$F4/80$^+$MHC-II$^+$) macrophages in the tumors from mice bearing Panc02 cells with miR-NC and miR-340 overexpression. (B) The ratio of M1-like and M2-like macrophages in the tumor microenvironment of tumor-bearing mice. (C) The proportion and MFI of M1-like (CD11b$^+$F4/80$^+$MHC-II$^+$) macrophages in the spleens from mice bearing Panc02 cells with miR-NC and miR-340 overexpression. (D) The ratio of M1-like and M2-like macrophages in the spleens of tumor-bearing mice. (E) The frequencies of CD4$^+$ T cells in the tumor microenvironment, (F) the frequencies of CD8$^+$ T cells in the tumor microenvironment, (G) the frequencies of CD4$^+$ T cells in the spleen, (H) the frequencies of CD8$^+$ T cells in the spleen, (I) the frequencies of CD4$^+$ T cells in the blood and (J) the frequencies of CD8$^+$ T cells in the blood in mice bearing Panc02 cells with miR-NC and miR-340 overexpression. (K) The orthotopic model of PDAC was established, and tumor-bearing mice were treated with isotype control mouse IgG or an anti-mouse *CD47* antibody. Representative plots and statistical analysis showed the percentage of F4/80$^+$GFP$^+$ macrophages phagocytosing cancer cells among macrophages with or without anti-*CD47* antibody blockade *in vivo*. The error bars were shown as mean±SEM and the data were analyzed by two-tailed, unpaired t-test. *P<0.05; **p<0.01 and ***p<0.001. PDAC, pancreaticductal adenocarcinoma.

upregulated in the miR-340- overexpressing tumors

(figure 5F). In the spleens from the tumor-bearing mice, both CD4$^+$ T lymphocytes and CD8$^+$ T lymphocytes were significantly upregulated in the miR-340 overexpression groups (figure 5G,H). In the blood from the tumor-bearing mice, although the CD4$^+$ T lymphocytes showed no statistically significant difference between the miR-NC and miR-340 stable overexpression Panc02 cell-bearing mice (figure 5I), the CD8$^+$ T lymphocytes were significantly upregulated in the miR-340-overexpressing mice (figure 5J), which was consistent with the results obtained in the tumors and spleens. In addition, to further demonstrate that miR-340 regulated phagocytosis by macrophages *in vivo*, we established an orthotopic model of PDAC and detected the changes in phagocytosis by macrophages using flow cytometry. An anti-*CD47* antibody was used as a positive control. Our research showed that the phagocytosis of macrophages increased significantly in miR-340-overexpressing tumor-bearing mice and further increased with *CD47* blocking (figure 5K), which showed that miR-340 could effectively enhance phagocytosis by macrophages *in vivo*.

Depletion of macrophages restores the inhibition of miR-340 leading to the tumor growth

To investigate whether macrophages contribute to the inhibitory effect of miR-340 on tumor formation by *CD47*-expressing cancer cells, we depleted mice of macrophages by administering clodronate liposomes prior to performing *in situ* injections of cancer cells into the pancreas throughout the experiment (figure 6A). The depletion of macrophages (CD11b$^+$F4/80$^+$) in the tumors was effective with an approximate decrease of 50% after the intravenous injection of clodronate liposomes (figure 6B,C) and clearly decreased after the intravenous injection of clodronate liposomes in the spleens (figure 6D,E). We found that clodronate liposome treatment partially inhibited tumor growth, but the combination had no additive effects on either tumor growth (figure 6F,G) or tumor weight (figure 6H), confirming that macrophages indeed contribute, at least partially, to the antitumor effect of miR-340. Therefore, considering our *in vitro* and *in vivo* studies, miR-340 directly inhibited the expression of *CD47*, resulting in the increased phagocytosis of tumor cells by macrophages, consequently enhancing antitumor immunity (figure 6I).

DISCUSSION

Tumor immune regulation is characterized by dynamic changes, which necessitates the discovery of new immune checkpoints and their ligands to provide a new mechanism for the antitumor immune response. In clinically successful treatments of several cancers, such as melanoma[30] and lung cancer,[31] the field of tumor immunology is rapidly developing. Anti-*CD47* has been proposed to both inhibit "self" signals and induce efficient uptake of cancer cells.[11] Antibodies targeting the *CD47–SIRPα* interaction in malignancies are currently studied in clinical
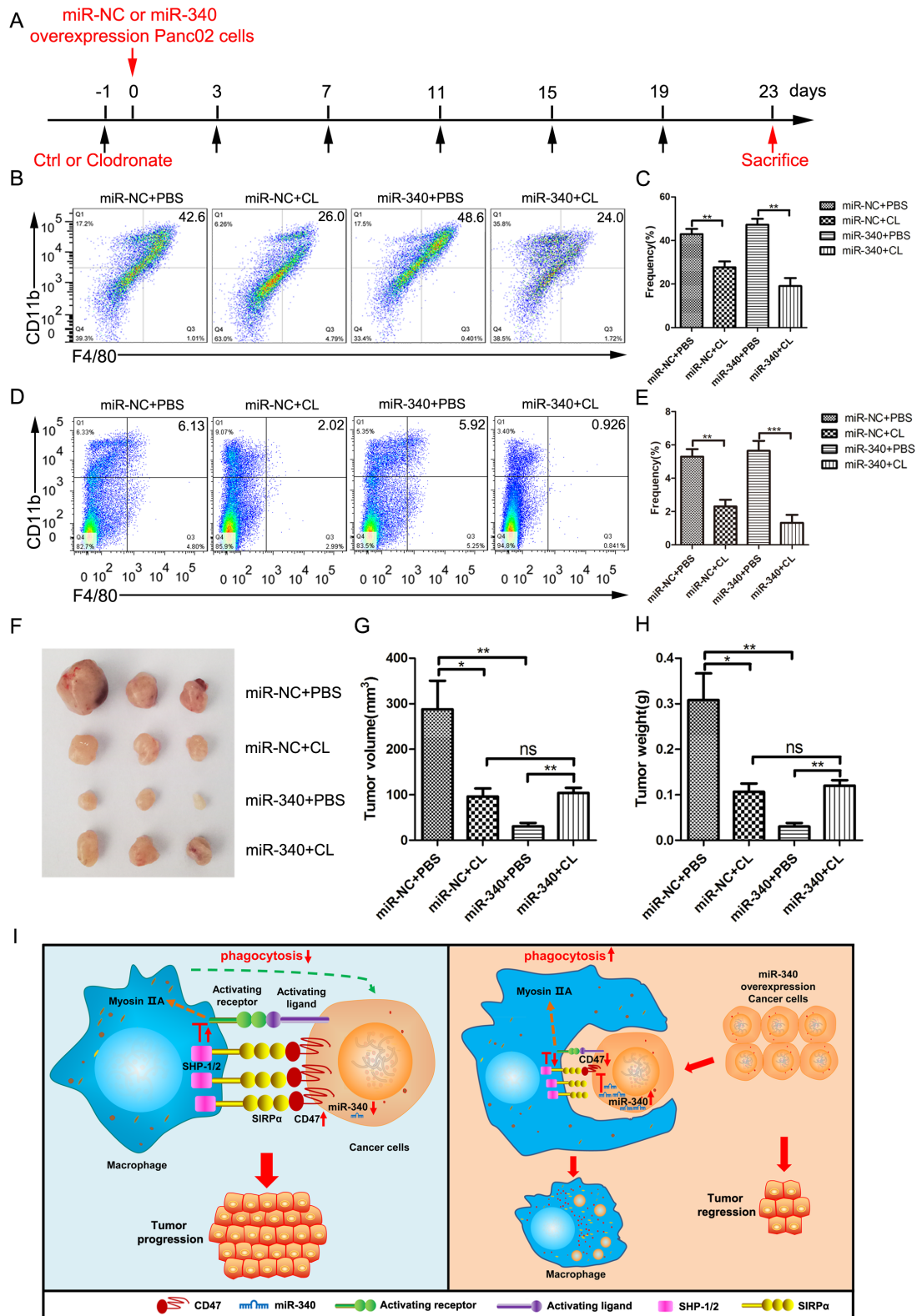
Figure 6 Macrophages mediated the antitumor effect of miR-340 against *CD47 in vivo*. C57BL/6 mice bearing Panc02 cells with miR-NC and miR-340 overexpression were injected intravenously with either PBS liposomes or clodronate liposomes at the indicated times (n=7 per group). (A) Schematic diagram of the macrophage depletion strategy. Immune cells isolated from tumors (B–C) and splenocytes (D–E) were stained with antibodies against CD45, CD11b and F4/80 for analysis by flow cytometry. The frequency of macrophages (CD11b+F4/80+) was expressed as a percentage of all CD45+ cells in each plot. (F) Representative images of tumors, (G) final tumor volumes and (H) final tumor weights in mice bearing Panc02 cells with miR-NC and miR-340 overexpression with or without macrophage depletion. (I) Schematic of the molecular mechanism by which miR-340 enhanced antitumor immunity. The error bars were shown as mean±SEM and the data were analyzed by two-tailed, unpaired t-test. *P<0.05; **p<0.01 and ***p<0.001.

trials, such as Hu5F9-G4[32] and ALX-148.[33] Although antibody-based treatment seems to be effective, the widespread expression of *CD47* increases the occurrence of side effects, such as temporary anemia[11] and neutropenia.[12] Moreover, these antibodies are large and possibly have limitations in tissue infiltration and recruitment of T cells to mediate effecter functions.[34] Recent studies showed novel antitumor therapy of targeting CD47 except for antibodies therapies. Intravenous injection of siRNA to reduce the expression of CD47 in cancer cells will render them targets for macrophage destruction.[35] MiRNA-based therapies complement miRNAs with tumor suppressive function by using synthetic double-stranded small miRNA mimics, can be chemically modified to delivery to tumors and consequently reinstate the lost miRNA expression in function. MiRNA mimics might be promising replenished therapies for the regulation of genes in cancer cells.[18 36] Strategies to improve the efficacy include miRNA mimics coupled to nanoparticles coated with tumor-specific antibodies,[37] systemically delivered neutral lipid emulsions of miRNA mimics,[38] formulations with atelocollagen to increase the efficient delivery of miRNAs into tumors[39] and engineered miRNA expression vectors that enable the expression of the miRNA of interest in a tissue-specific or tumor-specific manner.[40] With the deepening of research, promising low toxicity and payload delivery to target sites of miRNA mimics have been shown in several preclinical preparations.[41] Therefore, miRNA therapeutics may become a long-term clinical reality with the development of human biology and miRNA delivery vectors. Studies have shown that miR-708 regulates CD47 to inhibit phagocytosis by macrophages in T-cell acute lymphoblastic leukemia.[20] However, the study focused only on T-cell acute lymphoblastic leukemia, while our whole study is focused on one of the common solid tumor PDAC. We systematically evaluated the impact of miR-340 on the biological function of tumor cells, further analyzed the tumor immune microenvironment of an *in situ* pancreatic tumor model and confirmed that the restoration of miR-340 in cancer cells was sufficient to downregulate CD47 and promote phagocytosis by macrophages, ultimately inhibiting solid tumor growth.

Herein, we have shown that the expression of *CD47* in tumor tissues from patients with PDAC increased significantly compared with that in matched normal tissues. The high expression of *CD47* was closely related to poor prognosis in patients with PDAC. By using the LinkedOmics database, we found that the expression of miR-340 was inversely related to *CD47*, and the low expression of miR-340 was related to unfavorable prognosis in PDAC patients, highlighting the important role of miR-340 in PDAC. Previous studies have reported that miR-340 is silenced in several cancers and exerts a tumor-suppressive function in several cancers.[42 43] However, research investigating the regulatory effect of miR-340 in tumor immunity has been limited thus far. In our study, we determined that miR-340 directly binds the 3′ UTR and inhibits the expression of *CD47*. As the phagocytosis of tumor cells by macrophages increases with *CD47* blockade,[11] we investigated whether miR-340 could impact the function of macrophages through the miR-340–*CD47* axis. We found that the knockdown of *CD47* by miR-340 in cancer cells greatly enhanced the phagocytosis of tumor cells by macrophages *in vitro*. The orthotopic model of PDAC showed that the expression of *CD47* decreased in miR-340 overexpression tumor-bearing mice, and phagocytosis by macrophages increased significantly in miR-340 overexpression tumor-bearing mice and further increased with *CD47* blockade, which suggested that miR-340 regulated antitumor immunity by targeting *CD47 in vivo*. In addition, the depletion of macrophages attenuated the antitumor effect of miR-340, suggesting that the overexpression of miR-340 could prevent tumor formation partially by promoting phagocytosis of cancer cells by macrophages. Therefore, we found a new mechanism by which miR-340 regulates the *CD47* immune checkpoint, and targeting *CD47* by miR-340 may be a potential novel immunotherapeutic approach to the treatment of PDAC, which is characterized by high *CD47* expression levels.

We also investigated the effect of miR-340 on the immune microenvironment in peripheral immune organs and tumors formed by Panc02 cells stably overexpressing miR-NC or miR-340 in syngeneic mice. Given that tumor-associated macrophages (TAMs) are related to tumor progression and metastasis closely,[44] therapeutic options of targeting of *CD47* may have the potential to restore immunosurveillance and alter the role of macrophages in tumor immune microenvironment. In our research, the overexpression of miR-340 significantly inhibited tumor growth *in vivo*. The antitumor effect was miR-340-*CD47* dependent, enabling TAMs to phagocytose tumor cells. In the tumor microenvironment, TAMs acquired the properties of a polarized M2 phagocyte population, predominantly polarized toward an M2-like phenotype, which play critical roles in promoting the growth and progression of tumors.[45] A previous study showed that anti-*CD47* treatment alone could shift the phenotype of macrophages toward the M1-like subtype *in vivo* to play strong antitumor roles.[46] In our research, the suppression of tumor growth by miR-340 is likely achieved partially through the regulation of the M1-versus-M2 polarization of TAMs, leading to an obvious increase in the proportion of M1-like macrophages and an enhanced M1/M2 ratio in tumors, suggesting that miR-340 regulates the polarization of macrophages toward the M1-like state in the tumor microenvironment. We also found that the proportion of M1-like macrophages and the M1/M2 ratio were increased in the spleen, a peripheral immune organ, of mice bearing miR-340-overexpressing Panc02 cells. An important mode of communication between cancer cells and immune cells may occur through tumor-derived exosomes, which reprogram the functions of immune cells by delivering genomic DNA, mRNAs and miRNAs to them, induce immune cell dysfunction and silence antitumor immune responses and consequently promote

tumor progression.[47] A study has shown that miR-301a derived from tumor exosomes promotes pancreatic cancer metastasis through mediating M2 macrophage polarization.[48] Therefore, we speculated that the overexpression of miR-340 in cancer cells might be transferred to macrophages in peripheral immune organs, namely the spleen, through exosomes derived from cancer cells to promote antitumor immunity by mediating macrophage polarization with an unknown mechanism that needs further study. Previous studies have demonstrated that the efficacy of anti-*CD47* therapy against tumors requires adaptive immune responses in mouse tumor models.[49 50] As expected, the overexpression of miR-340 resulted in an increase in T cells, especially CD8$^+$T cells in the tumor, blood and spleen, likely because Panc02 cells with stable overexpression of the miR-340 became more effectively endocytosed by macrophages by the blockade of the CD47–SIRPα axis, which affected the phagocytic ability of macrophages, consequently enhancing the effectiveness of antitumor immunity.

CONCLUSIONS

In summary, we identified a tumor suppressive factor miR-340 that was negatively correlated with *CD47* expression. Our results indicated that miR-340 promotes macrophage phagocytosis by targeting *CD47* on pancreatic cancer cells, priming an effective antitumor T-cell response and consequently inhibiting tumor progression. Thus, treatment supplementing miR-340 may provide a complementary strategy to prevent the development and recurrence of PDAC.

Author affiliations
[1]Department of Immunology and Research Center of Basic Medical Sciences, Key Laboratory of Immune Microenvironment and Diseases of Educational Ministry of China, Tianjin Key Laboratory of Cellular and Molecular Immunology, Tianjin Medical University, Tianjin, China
[2]Guangdong Province Key Laboratory for Biotechnology Drug Candidates, School of Life Sciences and Biopharmaceutics, Guangdong Pharmaceutical University, Guangzhou, China
[3]Tianjin Key Laboratory of A cute Abdomen Disease Associated Organ Injury and ITCWM Repair, Institute of Integrative Medicines for Acute Abdominal Diseases, Nankai Hospital, Tianjin, China
[4]Department of Radiology, The University of Texas Southwestern Medical Center, Dallas, Texas, USA
[5]Guangdong Province Key Laboratory for Biotechnology Drug Candidates, School of Life Sciences and Biopharmaceutics, Guangdong Pharmaceutical University, Guangzhou, China; Department of Immunology and Research Center of Basic Medical Sciences, Key Laboratory of Immune Microenvironment and Diseases of Educational Ministry of China, Tianjin Key Laboratory of Cellular and Molecular Immunology, Tianjin Medical University, Tianjin, China

ORCID iD
Rongxin Zhang http://orcid.org/0000-0002-4083-374X

REFERENCES

1 Siegel RL, Miller KD, Jemal A. Cancer statistics, 2017. *CA Cancer J Clin* 2017;67:7–30.
2 Kamisawa T, Wood LD, Itoi T, *et al*. Pancreatic cancer. *Lancet* 2016;388:73–85.
3 Matlung HL, Szilagyi K, Barclay NA, *et al*. The CD47-SIRPα signaling axis as an innate immune checkpoint in cancer. *Immunol Rev* 2017;276:145–64.
4 Veillette A, Chen J. SIRPα-CD47 immune checkpoint blockade in anticancer therapy. *Trends Immunol* 2018;39:173–84.
5 Brown EJ, Frazier WA. Integrin-Associated protein (CD47) and its ligands. *Trends Cell Biol* 2001;11:130–5.
6 Kharitonenkov A, Chen Z, Sures I, *et al*. A family of proteins that inhibit signalling through tyrosine kinase receptors. *Nature* 1997;386:181–6.
7 Timms JF, Carlberg K, Gu H, *et al*. Identification of major binding proteins and substrates for the SH2-containing protein tyrosine phosphatase SHP-1 in macrophages. *Mol Cell Biol* 1998;18:3838–50.
8 Tsai RK, Discher DE. Inhibition of "self" engulfment through deactivation of myosin-II at the phagocytic synapse between human cells. *J Cell Biol* 2008;180:989–1003.
9 Weiskopf K, Jahchan NS, Schnorr PJ, *et al*. CD47-blocking immunotherapies stimulate macrophage-mediated destruction of small-cell lung cancer. *J Clin Invest* 2016;126:2610–20.
10 Michaels AD, Newhook TE, Adair SJ, *et al*. Cd47 blockade as an adjuvant immunotherapy for resectable pancreatic cancer. *Clin Cancer Res* 2018;24:1415–25.
11 Willingham SB, Volkmer J-P, Gentles AJ, *et al*. The CD47-signal regulatory protein alpha (SIRPa) interaction is a therapeutic target for human solid tumors. *Proc Natl Acad Sci U S A* 2012;109:6662–7.
12 Majeti R, Chao MP, Alizadeh AA, *et al*. Cd47 is an adverse prognostic factor and therapeutic antibody target on human acute myeloid leukemia stem cells. *Cell* 2009;138:286–99.
13 Bartel DP. MicroRNAs: genomics, biogenesis, mechanism, and function. *Cell* 2004;116:281–97.
14 Ha M, Kim VN. Regulation of microRNA biogenesis. *Nat Rev Mol Cell Biol* 2014;15:509–24.
15 Chen L, Gibbons DL, Goswami S, *et al*. Metastasis is regulated via microRNA-200/ZEB1 axis control of tumour cell PD-L1 expression and intratumoral immunosuppression. *Nat Commun* 2014;5:5241.
16 Hsieh C-H, Tai S-K, Yang M-H. Snail-overexpressing cancer cells promote M2-like polarization of tumor-associated macrophages by delivering MiR-21-Abundant exosomes. *Neoplasia* 2018;20:775–88.
17 Rupaimoole R, Calin GA, Lopez-Berestein G, *et al*. miRNA deregulation in cancer cells and the tumor microenvironment. *Cancer Discov* 2016;6:235–46.
18 Rupaimoole R, Slack FJ. MicroRNA therapeutics: towards a new era for the management of cancer and other diseases. *Nat Rev Drug Discov* 2017;16:203–22.
19 Suzuki S, Yokobori T, Tanaka N, *et al*. Cd47 expression regulated by the miR-133a tumor suppressor is a novel prognostic marker in esophageal squamous cell carcinoma. *Oncol Rep* 2012;28:465–72.
20 Huang W, Wang W-T, Fang K, *et al*. MIR-708 promotes phagocytosis to eradicate T-ALL cells by targeting CD47. *Mol Cancer* 2018;17:12.
21 Qin Y, Zhou X, Huang C, *et al*. Lower miR-340 expression predicts poor prognosis of non-small cell lung cancer and promotes cell proliferation by targeting CDK4. *Gene* 2018;675:278–84.

22 Huang K, Tang Y, He L, *et al*. MicroRNA-340 inhibits prostate cancer cell proliferation and metastasis by targeting the MDM2-p53 pathway. *Oncol Rep* 2016;35:887–95.

23 Kaneda MM, Messer KS, Ralainirina N, *et al*. Pi3Kγ is a molecular switch that controls immune suppression. *Nature* 2016;539:437–42.

24 Betel D, Wilson M, Gabow A, *et al*. The microRNA.org resource: targets and expression. *Nucleic Acids Res* 2008;36:D149–53.

25 Paraskevopoulou MD, Georgakilas G, Kostoulas N, *et al*. DIANA-microT web server v5.0: service integration into miRNA functional analysis workflows. *Nucleic Acids Res* 2013;41:W169–73.

26 Agarwal V, Bell GW, Nam J-W, *et al*. Predicting effective microRNA target sites in mammalian mRNAs. *Elife* 2015;4. doi:10.7554/eLife.05005. [Epub ahead of print: 12 Aug 2015].

27 Yang X-M, Cao X-Y, He P, *et al*. Overexpression of Rac GTPase activating protein 1 contributes to proliferation of cancer cells by reducing Hippo signaling to promote cytokinesis. *Gastroenterology* 2018;155:1233–49.

28 Vasaikar SV, Straub P, Wang J, *et al*. LinkedOmics: analyzing multi-omics data within and across 32 cancer types. *Nucleic Acids Res* 2018;46:D956–63.

29 Jaiswal S, Jamieson CHM, Pang WW, *et al*. Cd47 is upregulated on circulating hematopoietic stem cells and leukemia cells to avoid phagocytosis. *Cell* 2009;138:271–85.

30 Eggermont AMM, Chiarion-Sileni V, Grob J-J, *et al*. Prolonged survival in stage III melanoma with ipilimumab adjuvant therapy. *N Engl J Med* 2016;375:1845–55.

31 Borghaei H, Paz-Ares L, Horn L, *et al*. Nivolumab versus docetaxel in advanced Nonsquamous non-small-cell lung cancer. *N Engl J Med* 2015;373:1627–39.

32 Liu J, Wang L, Zhao F, *et al*. Pre-Clinical development of a humanized Anti-CD47 antibody with anti-cancer therapeutic potential. *PLoS One* 2015;10:e0137345.

33 Russ A, Hua AB, Montfort WR, *et al*. Blocking "don't eat me" signal of CD47-SIRPα in hematological malignancies, an in-depth review. *Blood Rev* 2018;32:480–9.

34 Chan AC, Carter PJ. Therapeutic antibodies for autoimmunity and inflammation. *Nat Rev Immunol* 2010;10:301–16.

35 Wang Y, Xu Z, Guo S, *et al*. Intravenous delivery of siRNA targeting CD47 effectively inhibits melanoma tumor growth and lung metastasis. *Mol Ther* 2013;21:1919–29.

36 Takahashi R-U, Prieto-Vila M, Kohama I, *et al*. Development of miRNA-based therapeutic approaches for cancer patients. *Cancer Sci* 2019;110:3976:1140–7.

37 Tivnan A, Orr WS, Gubala V, *et al*. Inhibition of neuroblastoma tumor growth by targeted delivery of microRNA-34a using anti-disialoganglioside GD2 coated nanoparticles. *PLoS One* 2012;7:e38129.

38 Trang P, Wiggins JF, Daige CL, *et al*. Systemic delivery of tumor suppressor microRNA mimics using a neutral lipid emulsion inhibits lung tumors in mice. *Mol Ther* 2011;19:1116–22.

39 Tazawa H, Tsuchiya N, Izumiya M, *et al*. Tumor-Suppressive miR-34a induces senescence-like growth arrest through modulation of the E2F pathway in human colon cancer cells. *Proc Natl Acad Sci U S A* 2007;104:15472–7.

40 Chen L, Zheng J, Zhang Y, *et al*. Tumor-Specific expression of microRNA-26a suppresses human hepatocellular carcinoma growth via cyclin-dependent and -independent pathways. *Mol Ther* 2011;19:1521–8.

41 Bader AG. miR-34 - a microRNA replacement therapy is headed to the clinic. *Front Genet* 2012;3:120.

42 Huang T, Zhou Y, Zhang J, *et al*. Srgap1, a crucial target of miR-340 and miR-124, functions as a potential oncogene in gastric tumorigenesis. *Oncogene* 2018;37:1159–74.

43 Fernandez S, Risolino M, Mandia N, *et al*. miR-340 inhibits tumor cell proliferation and induces apoptosis by targeting multiple negative regulators of p27 in non-small cell lung cancer. *Oncogene* 2015;34:3240–50.

44 Pollard JW. Tumour-educated macrophages promote tumour progression and metastasis. *Nat Rev Cancer* 2004;4:71–8.

45 Mantovani A, Sozzani S, Locati M, *et al*. Macrophage polarization: tumor-associated macrophages as a paradigm for polarized M2 mononuclear phagocytes. *Trends Immunol* 2002;23:549–55.

46 Zhang M, Hutter G, Kahn SA, *et al*. Anti-CD47 treatment stimulates phagocytosis of glioblastoma by M1 and M2 polarized macrophages and promotes M1 polarized macrophages *in vivo*. *PLoS One* 2016;11:e0153550.

47 Whiteside TL. Exosomes and tumor-mediated immune suppression. *J Clin Invest* 2016;126:1216–23.

48 Wang X, Luo G, Zhang K, *et al*. Hypoxic tumor-derived exosomal miR-301a mediates M2 macrophage polarization via PTEN/PI3Kγ to promote pancreatic cancer metastasis. *Cancer Res* 2018;78:4586–98.

49 Tseng D, Volkmer J-P, Willingham SB, *et al*. Anti-CD47 antibody-mediated phagocytosis of cancer by macrophages primes an effective antitumor T-cell response. *Proc Natl Acad Sci U S A* 2013;110:11103–8.

50 Soto-Pantoja DR, Terabe M, Ghosh A, *et al*. Cd47 in the tumor microenvironment limits cooperation between antitumor T-cell immunity and radiotherapy. *Cancer Res* 2014;74:6771–83.